Yale 耶鲁大学-南京信息工程大学大气环境中心

Yale-NUIST Center on Atmospheric Environment

A discussion of “Determination of area-averaged sensible heat fluxes with a large aperture scintillometer over a heterogeneous surface - Flevoland field experiment”.

Meijninger W M L et al., 2002.

Reporter: Wei Nan

2015.9.18

Outline

1 Introduction

2 Theory

3 Experimental Site and Measurements

4 Results and Discussions

5 Conclusions

1 Introduction

- So far, the observation of regional turbulence flux at the scales of a few to tens of kilometers is still very difficult, especially in the heterogeneous surface. In the last decades the scintillation method is proposed to attempt this question. The observation instrument based on this idea was later developed by the American NOAA wave propagation Laboratory.
- Large aperture scintillometer (LAS) has been used to determine the sensible heat and the latent heat fluxs. The LAS signal has to rely on the Monin– Obukhov Similarity Theory (MOST), while MOST requires horizontal homogeneity. So, the concept of blending height was drawn out.
- To test the applicability of the LAS over heterogeneous terrain, an intensive field experiment in Flevoland (The Netherlands) was conducted.

2 Theory

2.1 The scintillation method

The LAS consists of a transmitter and receiver device. The light emitted by transmitter can be effected by air fluctuations. The observed intensity fluctuations are analysed at the receiver side (σ^2_{lnA}), which can be expressed as the structure parameter of the refractive index of air C_n^2 . The relation between the path averaged $\langle C_n^2 \rangle$ and the variance of the logarithm of amplitude fluctuations is as follows:

$$\left\langle C_n^2 \right\rangle = 4.48\sigma_{\ln A}^2 D^{7/3} L^{-3}$$

Where D is aperture diameter, L is the path length.

When the wavelength ranges from visible light to near-infrared light, the effect of temperature to C_{n}^2 is largest. Here the concept of Bowen-ratio is used to build a relation between the structure of parameters of temperature C_T^2 and C_{n}^2.viz.

$$C_T^2 = C_{\mathrm{n}}^2 \left(\frac{T^2}{-0.78 \times 10^{-6} P} \right)^2 \left(1 + \frac{0.03}{\beta} \right)^{-2}$$

here P is the atmospheric pressure, T the absolute air temperature and β the Bowen-ratio. Here we evaluate the Bowen-ratio value applying the iterative method proposed by Green and Hayashi (1998)

$$\beta = \frac{H_{LAS}}{\langle R_{\mathrm{n}} \rangle - \langle G_s \rangle - H_{LAS}}$$

where the net radiation (R_n) and the soil heat flux (G_s) are area-averaged values.

Using MOST the sensible heat flux can be derived from C_n^2 and additional wind speed (u) data, viz.

$$\frac{C_T^2 \left(z_{LAS} - d\right)^{2/3}}{T_*^2} = f_{TT}\left(\frac{z_{LAS} - d}{L_{Ob}}\right)$$

with the Obukhov length $L_{Ob} = \frac{u_*^2 T}{g\kappa T_*}$ $\quad T_* = \frac{-H}{\rho c_p u_*}$

$$u_* = \frac{\kappa u}{\ln\left(\frac{z-d}{z_0}\right) - \psi_m\left(\frac{z-d}{L_{Ob}}\right)}$$

where ψ_m is the Businger–Dyer correction, g the gravitational acceleration, κ the von Kármán constant, ρ the density of air, c_p the specific heat of air at constant pressure, u_* the friction velocity, T_* the temperature scale, d the zero-displacement height and z_o the roughness length.

2.2 The concept of blending height applied to the LAS

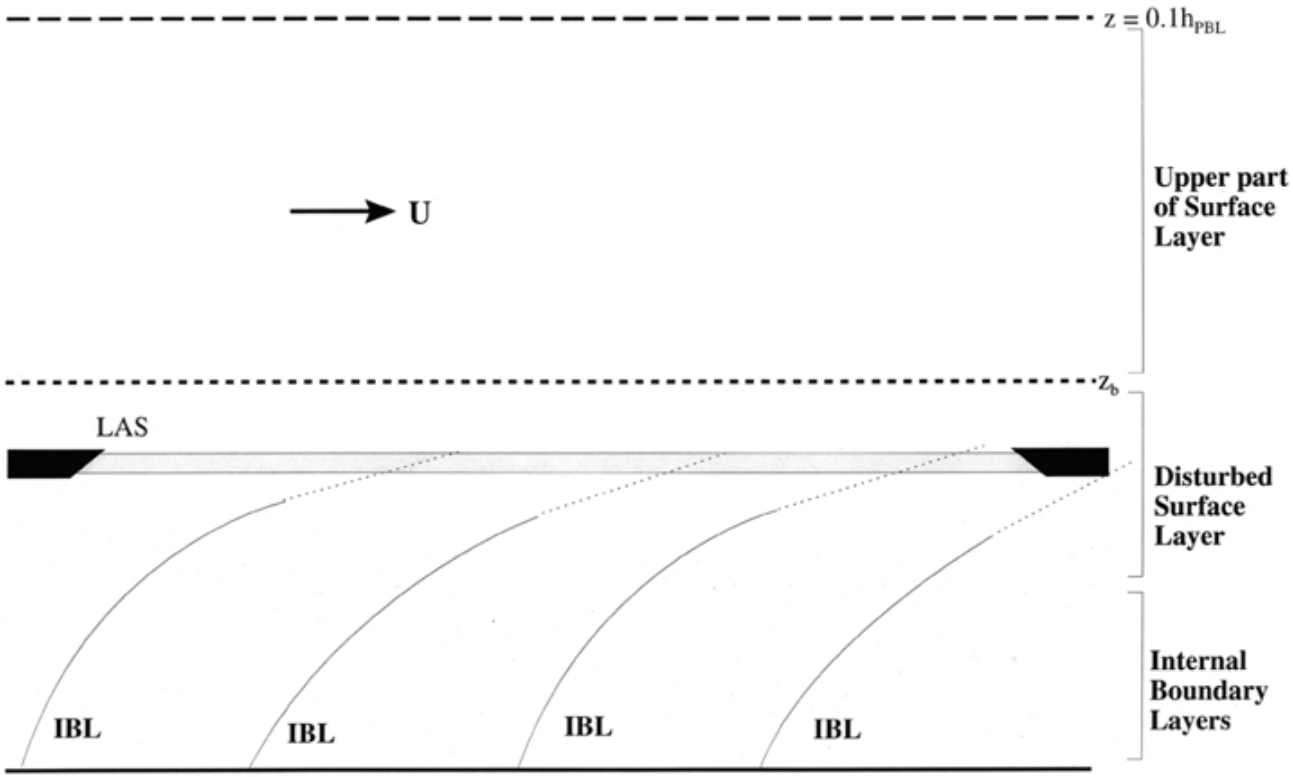

Figure 1. Schematic diagram of the various Layers over a heterogeneous flat landscape

Below the blending height, MOST might be violated.

2.3 The footprint concept applied to the LAS

A useful tool to determine the source area (SA) for turbulent fluxes is a footprint model.

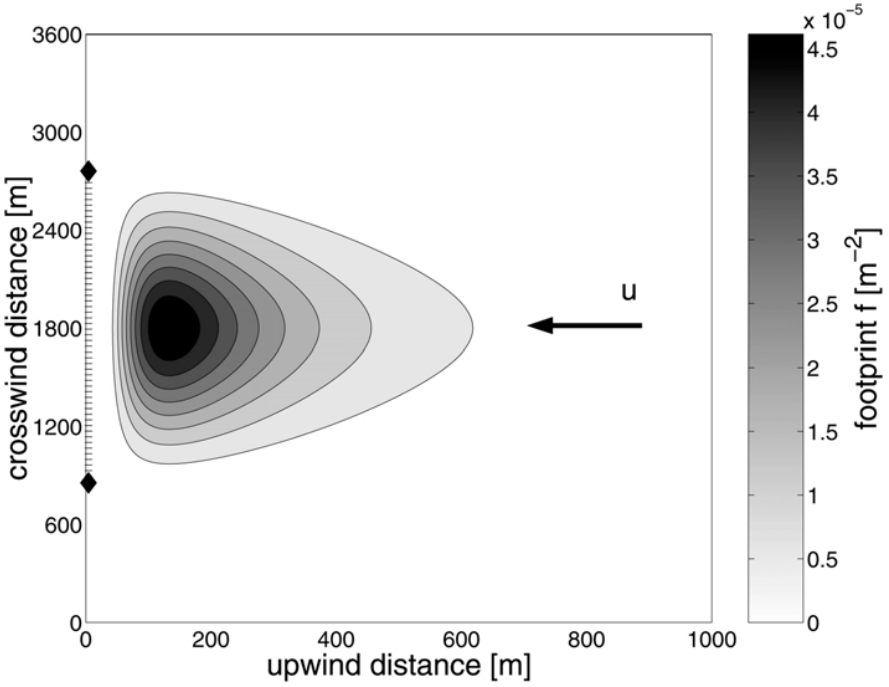

Figure 2a. The footprint (plan view) of a LAS where the wind direction is perpendicular to its path.

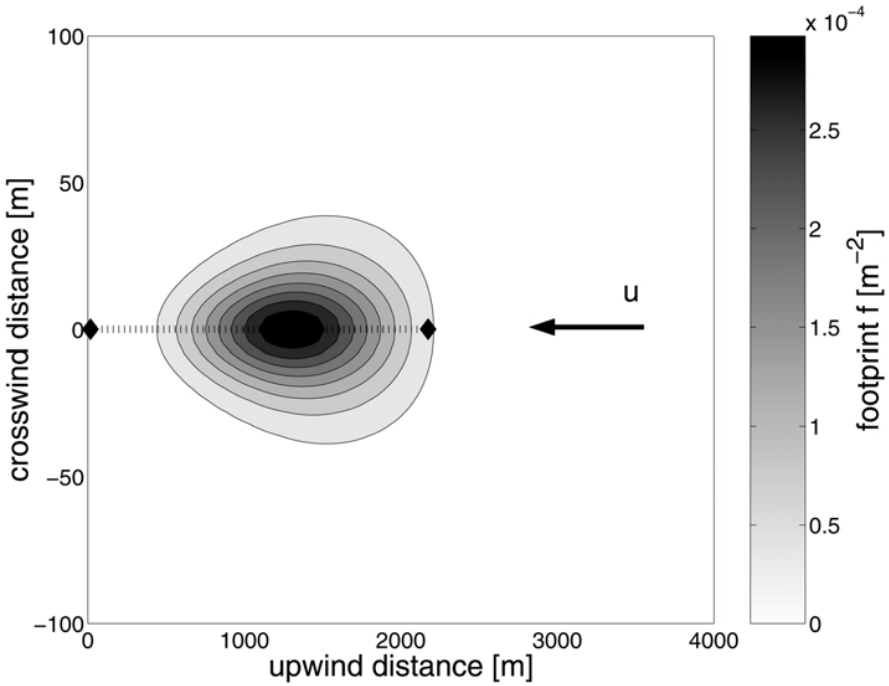

Figure 2b. As Figure 2a, the wind direction is parallel to the LAS's path.

3 Experimental site and measurements

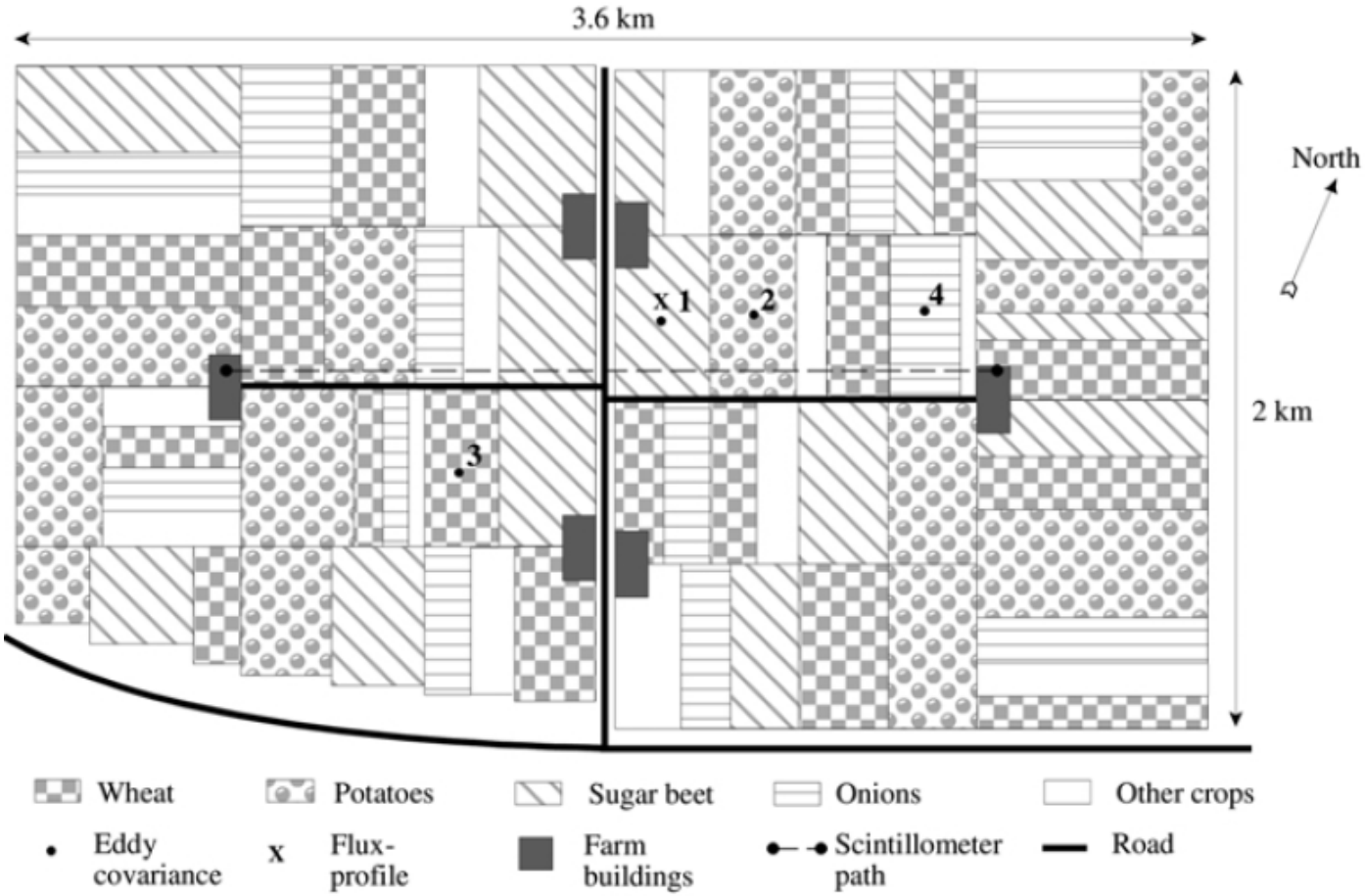

Site: Flevoland (The Netherlands, 52°22’51’’ N, 05°23’42’’ E). Observe period:18th July until the 20th August,1998.

Figure 3. A plan of the Flevoland area (denoted as area **A**) showing the vegetable plots.

TABLE I

Overview of instrumentation and the installed heights for each site.

Site	1: sugar beet	2: potatoes	3: wheat	4: onions
u, v, w and T_s	Solent R2 (4.8 m)	Solent R2 (3.6 m)	Solent R2 (3.5 m)	Solent R2 (2.8 m)
Temperature (T)	Thermocouple (4.8 m)	Thermocouple (3.5 m)	Thermocouple (3.5 m)	Thermocouple (2.8 m)
Humidity (q)	KH20 (4.8 m)	KH20 (3.5 m)	KH20 (3.5 m)	–
Net radiation (R_n)	Schulze–Däke (2.8 m)	Schulze–Däke (1.9 m)	Schulze–Däke (1.9 m)	Funk (1.6 m)
Soil heat flux (G_s) (at 0 mm)	WS31soil	WS31soil	WS31soil	Ws31soil
Wind speed (u)	Cup anemometer (3.9, 2.6 and 1.8 m)	–	–	–
Dry-bulb and wet-bulb (T, T & w)	Psychrometers (3.1 and 1.8 m)	–	–	–

4 Results and Discussions

4.1 The Eddy Covariance Results

TABLE II

Observed roughness lengths, crop heights and energy balance closure of eddy covariance measurements ($y = H + L_v E + G_s, x = R_n$).

	z_o [m]	h_{crop} [m]	Energy balance closure
Sugar beet	0.06	0.6–0.65	$y = 0.75x$, $R^2 = 0.84$
			RMS = 106 W m^{-2}
Potatoes	0.06	0.9–1.0	$y = 0.78x$, $R^2 = 0.86$
			RMS = 89 W m^{-2}
Wheat	0.06 (up to 10 August)	0.8–0.9 (up to 10 August)	$y = 0.91x$, $R^2 = 0.88$
	0.04 (after 11 August)	0 (after 11 August)	RMS = 56 W m^{-2}
Onions	0.05–0.06	0.5–0.65	–

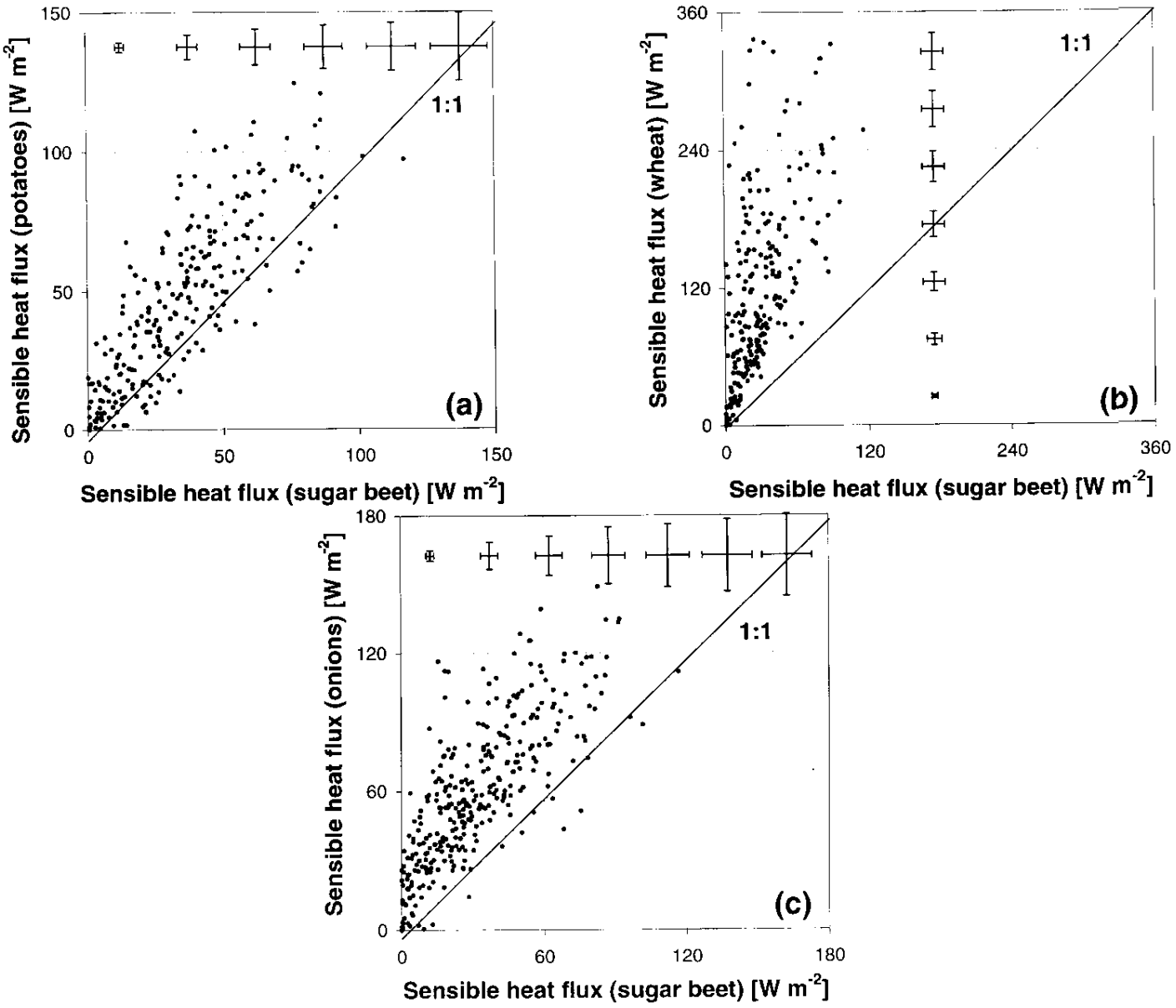

Figure 4. Comparison of the 30-min average eddy covariance measurements over the four plots. (a): Sensible heat fluxes over potatoes versus sugar beet. (b): Sensible heat fluxes over wheat versus sugar beet. (c): Sensible heat fluxes over onions versus sugar beet.

4.2 The Scintillometer Results

4.2.1 The influence of bleding height for LAS results

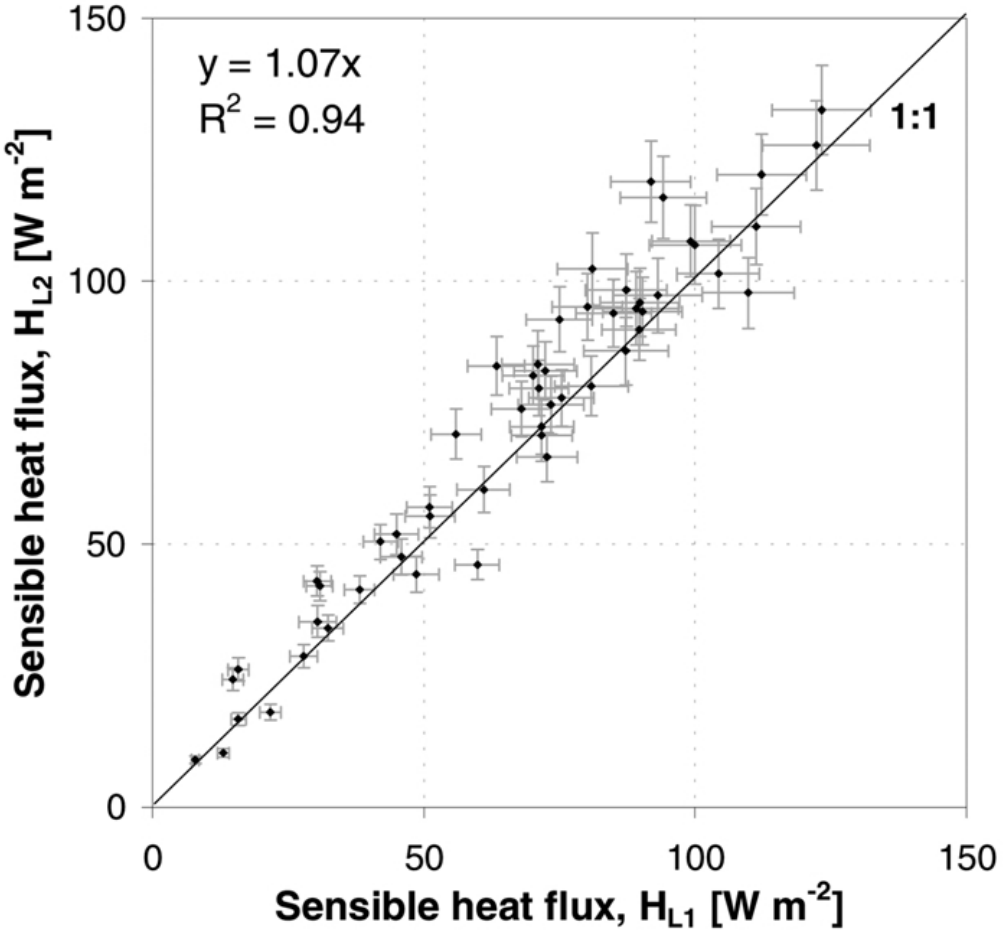

Figure 5. Comparison of 30-min measurements of sensible heat flux derived from LAS1 (H_{L1}) and LAS2 (H_{L2}).

4.2.2 The results comparison between LAS and EC

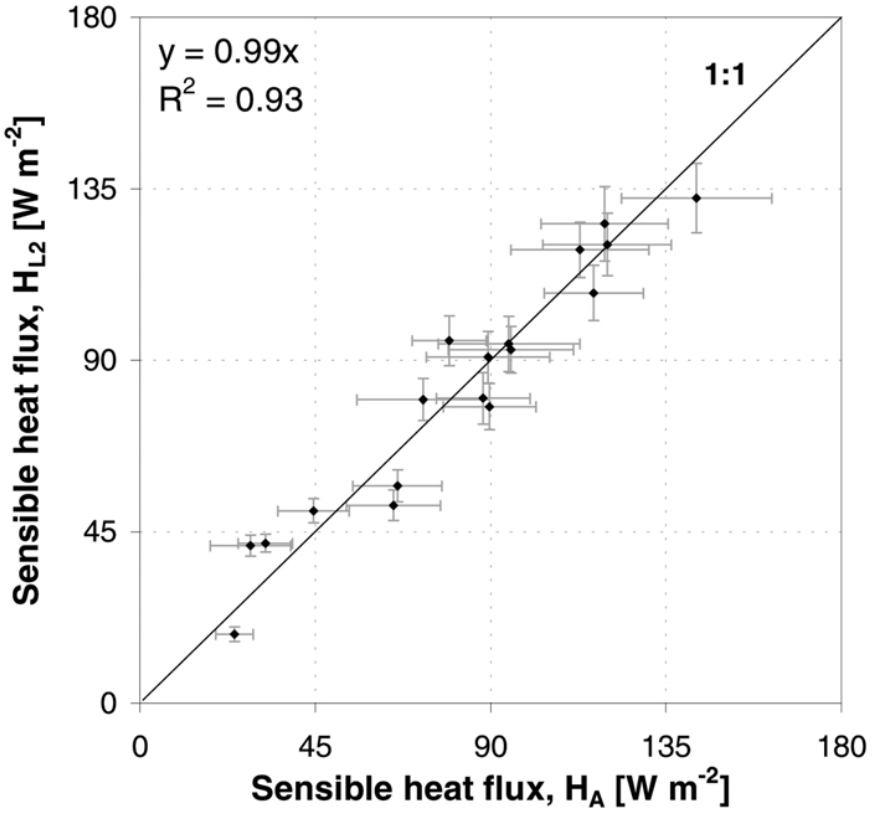

Figure 6. Comparison of 30-min fluxes of sensible heat derived from LAS2 (H_{L2}) and the area-averaged fluxes of sensible heat for area **A** (H_A) derived from eddy covariance measurements.

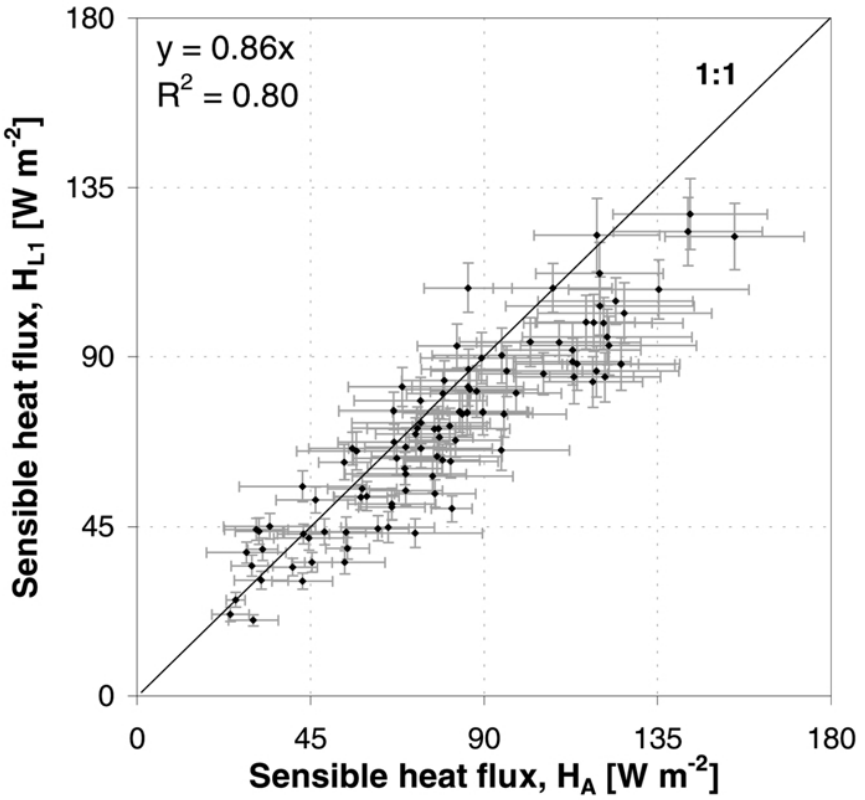

Figure 7. Comparison of 30-min fluxes of sensible heat derived from LAS1 (H_{L1}) and the area-averaged fluxes of sensible heat for area **A** (H_A) derived from eddy covariance measurements.

4.2.3 The footprint analysis to estimate the SA of the scintillometers.

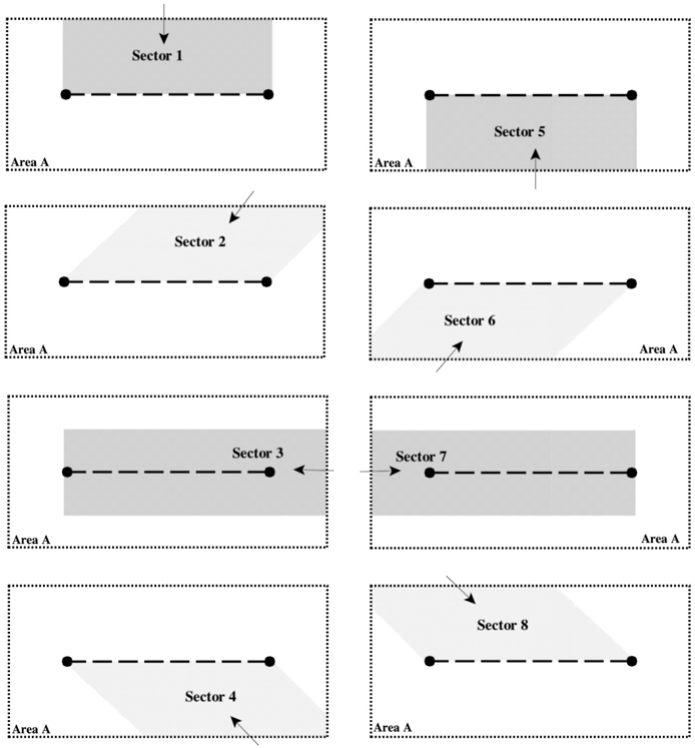

Figure 8. Division of area **A** in eight sectors based on three main wind directions, namely perpendicular, parallel and at an angle of 45 degrees to the path of the LAS.

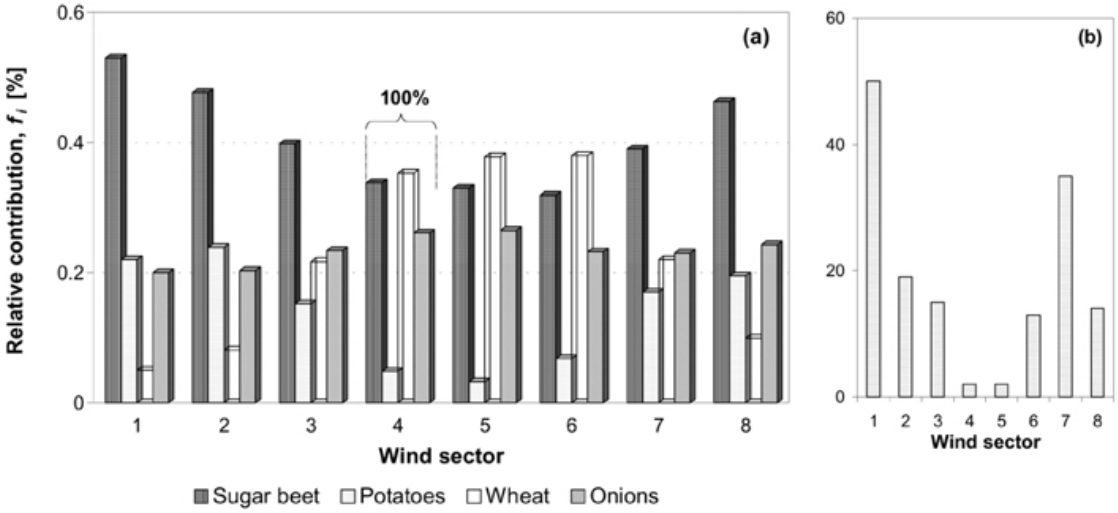

Figure 9. (a) The relative contribution of the four crops for each sector. The total contribution per sector is 100%. (b) Histogram of the observed wind direction during the experiment.

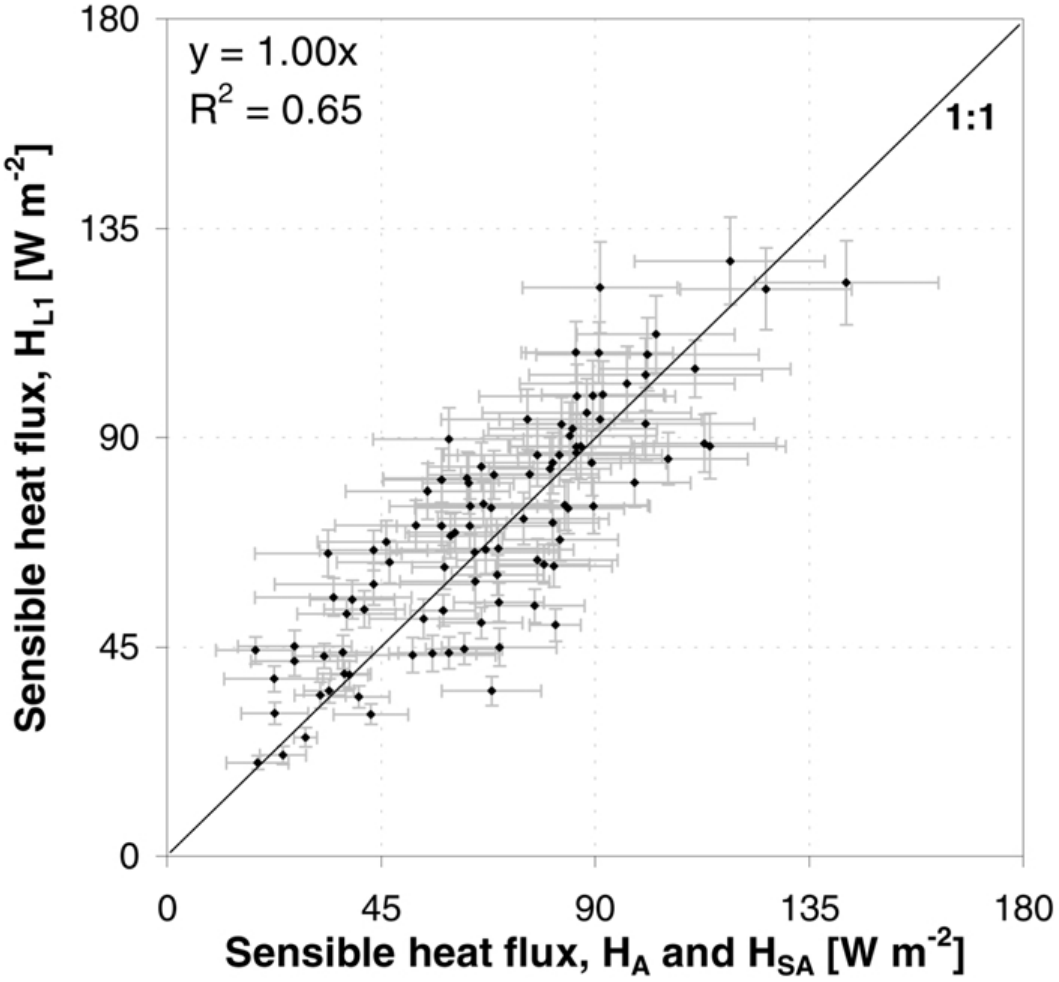

Figure 10. Comparison of 30-min fluxes of sensible heat derived from LAS1 (H_{L1}) and the area-averaged heat fluxes for area **A** (H_A) and the estimated source area (H_{SA}).

Conclusions

- LAS could be used to determine the heat flux over heterogeneous terrain.
- Using the Monin–Obukhov Similarity Theory (MOST), the fluxes derived from the LAS2 compared well with the area-averaged surface fluxes obtained from in-situ eddy covariance measurements. And below the blending height the results from LAS1 make clear that the violation of MOST is small.
- The footprint model of analysing the SA indicate that if the scintillometer is perpendicular to the main wind direction, the SA is maximum. And considering the SA and the spatial flux distribution, the result of LAS1 will be more reasonable.

Yale 耶鲁大学-南京信息工程大学大气环境中心

Yale-NUIST Center on Atmospheric Environment

Thank you for your attention!